



ALMA MATER STUDIORUM
UNIVERSITÀ DI BOLOGNA

ARCHIVIO ISTITUZIONALE
DELLA RICERCA

Alma Mater Studiorum Università di Bologna Archivio istituzionale della ricerca

Hollow-fiber flow field-flow fractionation and multi-angle light scattering investigation of the size, shape and metal-release of silver nanoparticles in aqueous medium for nano-risk assessment

This is the final peer-reviewed author's accepted manuscript (postprint) of the following publication:

Published Version:

Hollow-fiber flow field-flow fractionation and multi-angle light scattering investigation of the size, shape and metal-release of silver nanoparticles in aqueous medium for nano-risk assessment / Marassi, Valentina; Casolari, Sonia; Roda, Barbara; Zattoni, Andrea; Reschiglian, Pierluigi; Panzavolta, Silvia; Tofail, Syed A.M.; Ortelli, Simona; Delpivo, Camilla; Blosi, Magda; Costa, Anna Luisa. - In: JOURNAL OF PHARMACEUTICAL AND BIOMEDICAL ANALYSIS. - ISSN 0731-7085. - STAMPA. - 106:(2015), pp. 92-99. [10.1016/j.jpba.2014.11.031]

This version is available at: <https://hdl.handle.net/11585/555438> since: 2016-07-18

Published:

DOI: <http://doi.org/10.1016/j.jpba.2014.11.031>

Terms of use:

Some rights reserved. The terms and conditions for the reuse of this version of the manuscript are specified in the publishing policy. For all terms of use and more information see the publisher's website.

This item was downloaded from IRIS Università di Bologna (<https://cris.unibo.it/>).
When citing, please refer to the published version.

(Article begins on next page)

This is the final peer-reviewed accepted manuscript of:

MARASSI, VALENTINA; CASOLARI, SONIA; RODA, BARBARA; ZATTONI, ANDREA; RESCHIGLIAN, PIERLUIGI; PANZAVOLTA, SILVIA; TOFAIL, SYED A. M.; ORTELLI, SIMONA; DELPIVO, CAMILLA; BLOSI, MAGDA; COSTA, ANNA LUISA. Hollow-fiber flow field-flow fractionation and multi-angle light scattering investigation of the size, shape and metal-release of silver nanoparticles in aqueous medium for nano-risk assessment. *Journal of Pharmaceutical and Biomedical Analysis* 106, 92-99, 2015.

The final published version is available online at:
<http://dx.doi.org/10.1016/j.jpba.2014.11.031>

Rights / License:

The terms and conditions for the reuse of this version of the manuscript are specified in the publishing policy. For all terms of use and more information see the publisher's website.

This item was downloaded from IRIS Università di Bologna (<https://cris.unibo.it/>)

When citing, please refer to the published version.

1 Hollow-Fiber Flow Field-Flow Fractionation and Multi-Angle Light Scattering Investigation
2 of the Size, Shape and Metal-Release of Silver Nanoparticles in Aqueous Medium for
3 Nano-risk Assessment

4

5 Valentina Marassi¹, Sonia Casolari¹, Barbara Roda^{1,2,*}, Andrea Zattoni^{1,2}, Pierluigi
6 Reschiglian^{1,2}, Silvia Panzavolta¹, Tofail Syed³, Simona Ortelli⁴, Camilla Delpivo⁴, Magda
7 Blosi⁴, Anna Luisa Costa⁴

8 *¹Department of Chemistry "G. Ciamician", Via Selmi 2, 40126 Bologna, Italy, and*

9 *²byFlow Srl, Via Caduti della Via Fani 11/b, 40127 Bologna*

10 *³Department of Physics & Energy, University of Limerick, Ireland*

11 *⁴Institute of Science and Technology for Ceramics (CNR-ISTEC), National Research
12 Council of Italy, Via Granarolo 64, 48018 Faenza, RA, Italy*

13

14

15

16

17

18

19

20 *corresponding author: Barbara Roda phone: +390512099581

21 email: barbara.roda@unibo.it

22 ABSTRACT

23 Due to the increased use of silver nanoparticles in industrial scale manufacturing,
24 consumer products and nanomedicine, reliable measurements of the size, shape and
25 distribution of these particles in aqueous medium is critical since these properties affect
26 both functional properties and biological impact especially in quantifying associated risks
27 and identifying suitable risk-mediation strategies. The feasibility of an on-line coupling of a
28 fractionation technique such as hollow-fiber flow field flow fractionation (HF5) with light
29 scattering techniques such as MALS (multi-angle light scattering) have been investigated
30 for this purpose and data obtained have been compared with those from more
31 conventional, but often complementary techniques e.g. transmission electron microscopy,
32 dynamic light scattering, atomic absorption spectroscopy, and X-ray Fluorescence. The
33 combination of fractionation and multi angle light scattering techniques have been found to
34 offer an ideal, hyphenated methodology for the simultaneous size-separation and
35 characterization of silver nanoparticles. The hydrodynamic radii determined by
36 fractionation techniques can be conveniently correlated to the mean average diameters
37 determined by multi angle light scattering and reliable information on particle morphology
38 in aqueous dispersion can be obtained. The ability to separate silver (Ag^+) ions from the
39 silver nanoparticles (AgNPs) via membrane filtration during the size analysis can be an
40 added advantage in obtaining quantitative insights to its risk potential. Most importantly,
41 the methodology developed in this article can potentially be extended to similar
42 characterization of metal-based nanoparticles when studying the functional effectiveness
43 and potential hazards of these nanoparticles.

44

45 Keywords:

46 Ag nanoparticles in nanomedicine, HF5 size analysis of AgNPs, HF5-MALS of metal
47 nanoparticles, HF5 conformational studies of metal nanoparticles, HF5 metal release
48 analysis of AgNPs, HF5 for nanorisk assessment

49

50 **1. INTRODUCTION**

51 Nanoparticles are interesting tools for various applications [1]. Thanks to their high
52 surface/volume ratio, they present a noticeably different activity with respect to that of
53 smaller compounds .

54 Sustainable development of the nanotechnologies, as well as in other relevant industrial
55 applications must avoid any adverse effect on health of humans and environment exposed
56 to nanomaterials, thus justifying a close attention to safety issues. In particular, the
57 novel/revived attention on colloidal silver antimicrobial applications, used in food
58 packaging materials, food supplements, odor-resistant textiles, household appliances,
59 cosmetics and medical devices, water disinfectants, and room sprays applications,
60 addresses to AgNPs the attention of European nano-safety research [2],[3]. Such
61 relevance is also justified by the fact that surface engineered metal nanoparticles find their
62 use also as therapeutic agents in drug delivery applications; moreover, their dimensions
63 match that of biological building blocks, from proteins to organelles, leading to question
64 about interactions with living organisms [4][5]. The use of nanoparticles as drug carrier
65 may reduce the toxicity of the incorporated drug and the toxicity of the whole formulation is
66 investigated. However, results of the nanoparticles alone are not often described, and a
67 discrimination between drug and nanoparticle toxicity cannot be made. A specific
68 emphasis on the toxicity of the “empty” non-drug loaded particles is instead particularly
69 important when slowly or non degradable particles (as metal nanoparticles) are used for
70 drug delivery since they might show persistence and accumulation on the site of the drug
71 delivery, eventually resulting in chronic inflammatory reactions.

72 The development of safer by design nanomaterials, based on surface engineering could
73 effectively represent an inherent safety approach, able to design out hazard at the source.
74 Nevertheless, to ensure the effectiveness of such preventive measures, it is necessary to
75 perform a deep characterization of physicochemical properties, affecting biological and
76 functional properties, while a solid comprehension of mechanism leading nanoparticles
77 biological reactivity is required. In particular, the discrimination between different hazard
78 determining factors within and outside the complex biological matrix is fundamental in
79 order to establish strategies that can mitigate the risk. Such a goal is particularly important
80 when toxicity assessment of silver colloidal systems is addressed, since there is still an
81 ongoing debate about the mechanism by which AgNPs exert toxicity, and its consequential
82 antimicrobial effect [6]. Despite the common accepted mechanism for which the release of
83 cationic Ag represents the primary mechanism of antibacterial action, evidences of a
84 particle specific activity are also reported.

85 A technique able to perform the metal ions quantification and the characterization of silver
86 nanoparticles dispersed in aqueous media, is, for these reasons, strategic to better
87 elucidate biological interaction mechanism and develop solutions to decrease health
88 impact by preserving antibacterial activity [7]. Since most of the studies are conducted
89 over commercially available nanosilver having limited, if any, control over AgNPs' size,
90 morphology, degree of agglomeration and distribution between zerovalent (Ag^0) and
91 cationic Ag (Ag^+), free or adsorbed onto the surface, it is quite difficult to draw universally
92 accepted conclusions regarding the toxicity mechanism of nanosilver [8][9]. To investigate
93 how and if nanoparticles may present harm for the environment and organisms, a
94 characterization of their behavior in environmental/physiological medium is required
95 besides a characterization of their size, shape, activity and stability [10]. The most
96 common techniques used for NPs analysis in liquid media involve DLS (Dynamic Light
97 Scattering), chromophore counting, resonant light scattering and Raman scattering. High

98 resolution electron microscopy typically deals with the analysis of precipitates formed by
99 drying the colloidal solution on a microscopic grid and often involves a cross sectional cut.
100 DLS does not provide any information on particle shape and density distribution and its
101 accuracy may be intrinsically limited in particular when used in complex samples [11].
102 Static, multi-angle LS (MALS) gives independent information on the NP molar mass (M_r)
103 and root-mean-square (rms) radius values [12]. Consequently, it may provide information
104 on compactness and shape of the NPs. Hyphenation of DLS or MALS detection with size-
105 based separation methods represents a multidimensional platform that can then enhance
106 the accuracy of analysis of complex NPs samples.

107 Among separative techniques for nanodispersed analytes, Flow Field-Flow Fractionation
108 (F4) is increasingly employed as a mature separation method able to size-sort and isolate
109 NPs. Coupled with on-line uncorrelated detection methods including MALS, DLS,
110 absorbance and luminescence spectrophotometry, F4 is able to offer an multidimensional
111 analytical platform for nanomaterials analysis providing size distribution analysis,
112 identification of aggregation phenomena, separation of the unbound constituents of the
113 functional NPs, functional characterization of the NPs and correlation of spectroscopic
114 properties with NP size [13]. F4 is ideally suited to separate dispersed analytes over a
115 broad size range, from nanometer to micrometer sized analytes based on their coefficient
116 diffusion and dimensions [14]. In addition to size fractionation, in F4 membranes also act
117 as in-line sample micro-purification/desalting membranes during the focus/relaxation step
118 used for the sample injection. During the analysis, samples smaller than membrane cut-off
119 exit from it and can be collected from cross-flow line and analyzed using a technique able
120 to quantify them, such as flame absorption atomic spectroscopy. F4 can be used in two
121 technical variants, the asymmetrical F4 (AF4) and the hollow fiber F4 (HF5). AF4 is the
122 most established technique for the analysis of structured NPs and it involves the use of a
123 rectangular capillary channel where one wall is constituted by an ultrafiltration membrane

124 to allow the passage of a cross-flow [15][16][17][18].The quantitative determination of
125 metallic NPs using AF4 and MALS was already demonstrated for the characterization of
126 gold NPs [19][20], while AF4-UV and AF4-ICP were used to characterize standard Silver
127 nanoparticles [21]. Many applications of AF4 for NPs characterization in nanomedicine
128 were also reviewed [22 and references therein] .

129 HF5 is the miniaturized variant of the F4 technique and its use in the field of protein
130 analysis have been widely reported [23]; on the other hand, methods for NPs
131 characterization were still unexplored.

132 In HF5, the separation channel has a cylindrical geometry and consists in a HF membrane
133 with porous walls made of polymeric or ceramic materials and the separation is performed
134 through an external hydrodynamic field (named cross-flow) applied perpendicularly to a
135 mobile phase flow with an ideally laminar (parabolic) flow profile (named longitudinal flow).

136 Sample components are hydrodynamically driven towards one wall (accumulation wall) of
137 the channel and they move away from the wall due to diffusion, which creates a
138 counteracting motion. Smaller particles, which have a higher diffusion coefficient, move
139 closer to the channel center where the longitudinal flow is faster. This results in an earlier
140 elution of smaller particles with respect to larger species. Due to the symmetry of the
141 channel geometry, the driving force of the separation in HF5 is represented by a radial
142 flow (hence cross-flow) applied perpendicularly to the migration flow (axial/longitudinal
143 flow) with a cross flow density higher than that of AF4, leading to an increase in separation
144 efficiency. Down-scaling of the separation channel has proven to have important intrinsic
145 features that lead to great potential in the bioanalytical field: the sample dilution is reduced
146 because of the low channel volume, and as a consequence sensitivity can be increased
147 [24][25][26] and sample fractions can be easily collected for further analysis; in addition,
148 diluted samples can be injected and re-concentrated in shorter time [27] [28].Moreover,
149 disposable usage of the separating channel eliminates sample carry-over or sample

150 contamination issues. Wyatt Technology Europe has recently commercialized Eclipse®
151 DUALTEC, instrumentation able to operate both with the HF5 and F4 with the same
152 system [29].

153 In this paper we describe a novel approach that combines HF5 with MALS for the size
154 analysis of AgNPs dispersed in water. Due to the increased use of silver nanoparticles,
155 analysis of potential residues and metabolites of these new pharmaceuticals in
156 environmental, food and clinical materials represents a challenging task. Since the
157 nanorisk is correlated to the nanoparticles dimension, shape and Ag⁺/Ag⁰ ratio, a method
158 based on HF5-MALS able to determine the shape of the dispersed AgNPs in aqueous
159 media and also to separate molar ion fraction to silver nanoparticles, was developed.

160 **2. MATERIAL AND METHODS**

161 **2.1 AgNPs sample**

162 Aqueous colloidal nanosuspension (nanosol) of silver-polyvinylpyrrolidone nanoparticles
163 (AgNPs 4 % wt) was provided by Colorobbia SpA (Italy).

164 **2.2 Standards**

165 Polystyrene nanoparticles (PS) of 50 nm and 102 nm diameter (Nanosphere Size
166 Standards, Duke Scientific Corp.) were used as standards for the conformational analysis;
167 since they are spherical and their structure can be assimilated to that of a random coil, a
168 radius of gyration (r_g)/hydrodynamic radius (r_h) ratio of 0.77 is estimated. Thus the
169 standards' calculated r_g are respectively 20 nm and 43 nm.

170 **2.3 AgNPs Ultrafiltration**

171 Ultrafiltration was carried out using Solvent-resistant Stirred Cell (Merck Millipore) with
172 polymeric membrane with a pore size of 100 kDa, which was kept in slight overpressure
173 (about 3 bar). The ultrafiltration system was able to retain AgNPs, while the solvent of
174 nanosol containing synthesis by-products and cationic silver (Ag⁺) was removed. The

175 vessel refilled with deionized water was treated for four times until the total removal of free
176 cationic Ag⁺.

177 **2.4 HF5-MALS instrumental setup**

178 HF5 was performed by using an Agilent 1200 HPLC system (Agilent Technologies, Santa
179 Clara, CA, USA) consisting in a degasser, an isocratic pump, an autosampler and a
180 variable wavelength UV detector, combined with an Eclipse® DUALTEC separation
181 system (Wyatt Technology Europe, Dernbach, Germany).

182 The HF5 channel (Wyatt Technology Europe) consisted of two sets of ferrules, gaskets
183 and cap nuts used to seal a polymeric hollow fiber inside a plastic cartridge. The scheme
184 of the HF5 cartridge, its assembly and the modes of operation of the Eclipse® DUALTEC
185 system have already been described elsewhere [24]. The hollow fiber was a polyether-
186 sulfone (PES) fiber, type FUS 0181 available from Microdyn-Nadir (Wiesbaden, Germany)
187 with the following characteristics: 0.8 mm ID, 1.3 mm OD, and 10 kDa M_w cut-off,
188 corresponding to an average pore diameter of 5 nm. The HF5 channels used for the
189 experimental were a standard cartridge containing a 17 cm long fiber.

190 The ChemStation version B.04.02 (Agilent Technologies) data system for Agilent
191 instrumentation was used to set and control the instrumentation and for the computation of
192 various separation parameters. The software package Wyatt Eclipse @ ChemStation
193 version 3.5.02 (Wyatt Technology Europe) was used to set and control the flow rate values
194 and to move the focus position during the sample focus/concentration.

195 A 18-angle multiangle light scattering detector model DAWN HELEOS (Wyatt Technology
196 Corporation, Santa Barbara, CA, USA) operating at a wavelength of 658 nm, was used to
197 measure the radius of particles in solution. An Optilab rEX differential refractive index (dRI)
198 detector (Wyatt Technology Corporation) operating at a wavelength of 658 nm was used
199 on occasion as a concentration detector, when the capabilities of the UV detector were
200 overcome by the complexity of the sample. ASTRA® software version 5.3.2.14 (Wyatt

201 Technology Corporation) was used to handle signals from the detectors (MALS, dRI and
 202 UV) and to compute the protein M_w and concentration values.

203 **2.5 HF5 methods**

204 An HF5 method is composed of few steps: focus, focus-injection, elution and elution-
 205 injection. During focus the mobile phase is split into two different streams entering from the
 206 fiber's inlet and outlet; during focus-injection, the flow settings are the same described in
 207 the focus step while the sample is introduced into the channel through the inlet and
 208 focalized in a narrow region. Then, in the elution step, the flow of mobile phase enters the
 209 channel inlet and part of it comes out transversely (cross-flow); lastly, during elution-
 210 injection, no cross-flow is applied (the flow is not split anymore), allowing for any remaining
 211 sample inside the channel to be released; also, the flow is redirected in the injection line
 212 as well to clean it before the next injection.

213 The flow conditions for the different HF5 analysis are shown in Table 1. Longitudinal flow
 214 is indicated as V_c , while cross/focus flow as V_x . In flow-injection analyses (FIA) neither
 215 focus nor cross-flow are applied, thus allowing all injected analytes to exit from the
 216 channel without retention.

217 A volume of AgNPs of 4 μ L was injected.

218

219 *Table 1. Flow conditions for F4 analyses*

Steps → ↓Method	Focus (mL/min)	Focus-injection (mL/min)	Elution (mL/min)	Elution-injection (mL/min)
HF5	$V_c=0.35$ $V_x=0.85$ Time=2 min	$V_c=0.35$ $V_x=0.85$ Time=3 min	$V_c=0.35$ $V_x=0.1$ Time=12 min	$V_c=0.35$ $V_x=0$ Time=3 min
FIA	-	-	-	$V_c=0.5$ $V_x=0$ Time=3 min

cationic Ag collection	-	Vx=1 Vc=0 Time=12 min	-	-
------------------------	---	-----------------------------	---	---

220 **2.6 AgNPs size characterization**

221 2.6.1 DLS analysis

222 AgNPs size distribution was determined at room temperature by Zetasizer Nanoseries
 223 (Malvern Instruments, UK) providing the hydrodynamic diameter of suspended particles by
 224 the DLS technique. The hydrodynamic diameter was expressed as D50, i.e. the median
 225 diameter at 50% in the cumulative distribution. DLS analysis also provides a polydispersity
 226 Index parameter (PDI), ranging from 0 to 1, quantifying the colloidal dispersion degree. PDI
 227 values smaller than 0,05 are typical of highly monodispersed standards, while values
 228 greater than 0,7 depict a broad particle size distribution that makes samples unsuitable for
 229 DLS analysis. A mid-range PDI value between 0,05 and 0,7 usually ensures a proper
 230 operating condition of the instrument. As for DLS analysis, AgNPs were dispersed in
 231 deionized water at 0.13 mg/ml and homogenized on a vortex mixer for 30 seconds; the
 232 resulting dispersion pH was 4,5. A small sample volume (~1 mL) was subjected to three
 233 consecutive measurements performed at 25° C and particle size distribution by intensity
 234 was obtained by averaging these measurements.

235 2.6.2 TEM morphological investigation

236 The observation of morphology was made using a transmission electron microscope
 237 (TEM) in JEOL JEM-2100F multipurpose, high resolution, electron microscope with a field
 238 emission source operating between 80 and 200 kV for various level of magnifications. The
 239 nanoparticles were taken directly from the ultrafiltered nanosol and placed on TEM grids.
 240 The samples were then left to dry before loading in the TEM. Particle size and distribution
 241 were determined using image processing software on micrographs taken at around 200 kV
 242 emission field on multiple locations within the sample.

243 **2.7 Cationic Ag determination in NPs samples**

244 2.7.1 FAAS analysis

245 An AAnalyst400 (Perkin Elmer, Massachusetts, USA) flame atomic absorption
246 spectrometer (FAAS) equipped with a silver hollow-cathode-lamp, operating at 328.0 nm,
247 was used for quantitative analyses of solutions collected from the HF5 cross-flow line. The
248 instrumental parameters (10 mA operating current, 2.7 nm bandwidth) were adjusted
249 according to the manufacturer's recommendations. Air (10 ml/min)-C₂H₂ (2.5 ml/min) flame
250 was employed. Ultrapure MilliQ water and nitric acid 0.5M (HNO₃ for trace analysis, ≥69%,
251 Fluka) were used to dilute samples or standards in all the experiments.

252 Silver standard solutions, ranging from 0.2 mg/L to 5.0 mg/L, for FAAS calibration curve
253 were obtained by properly diluting a certificate solution of Ag (1002 ±2) mg/L (Merck,
254 Germany). The calibration curve, achieved under the best instrumental conditions, shows
255 a good linear correlation ($R^2 = 0.9972$). The equation $Y = 0.0211 (\pm 0.0003) X + 0.0040 (\pm$
256 $0.0009)$ was obtained when repeating the calibration 14 times.

257 2.7.2 HF5 filtration of AgNPs – proof of concept

258 The Inductively Coupled Plasma (ICP) analysis of aqueous colloidal nanosuspension of
259 the AgNPs characterized in this work estimates the total silver amount in 4% w/v. A part of
260 this silver amount is present in its ionic form and during the focus-inject step of HF5
261 analysis it passes through hollow fiber pores and can be collected and quantified.
262 Therefore as a proof of concept, solutions having cationic Ag concentrations of the same
263 order of magnitude as those presumably contained in AgNPs' nanosol were first injected into the hollow
264 fiber channel. The flows were selected in order to collect ionic silver from the cross-flow line
265 during the focus-inject step according to Table 1. During HF5 analysis the sample is
266 diluted almost 1:10, hence we suppose that the nanosol injected could be in the order of
267 4000 ppm in Ag. In order to determine the best volume to collect from the cross-flow line, 10
268 µL of a solution of AgNO₃ (1904 ppm) were injected into the HF5 system. This solution is
269 prepared by diluting 1:2 a stock solution of 3908 ppm, obtained by dissolving 59.94 mg (± 0.01)

270 mg of AgNO₃ in 10 ml of HNO₃ 0.5M. Five 3 ml aliquots were collected from the cross
271 flow line and analyzed by FAAS. For each of these aliquots, the concentration of silver
272 was obtained by interpolating the absorbance signal on the calibration curve.

273 2.7.3 XRF

274 From the ultrafiltered sample the concentration of cationic Ag present in water filtrates was
275 estimated by XRF (WDS - wavelength dispersive X-ray spectrometer) using a Panalytical
276 Axios Advanced (Netherlands). The XRF results showed that the ultrafiltration process
277 allowed removal of 50% of Ag (compared to the initial total amount of Ag), until reaching a
278 plateau, corresponding to the amount of cationic Ag at equilibrium with Ag⁰ solid phase.
279 The results showed that about 50% of Ag nanosol consists of nanoparticles and the
280 remaining 50% is made of cationic Ag.

281

282 3. RESULTS AND DISCUSSION

283 First we developed methods for the size-fractionation of AgNPs which are robust and
284 reproducible, and able to detect AgNPs in aqueous media with a satisfactory sensitivity in
285 particular with HF5.

286 3.1 HF5- MALS of AgNPs

287 Sample was separated in HF5 using water as mobile phase in order to analyze samples in
288 their native formulation and to avoid potential modification due to fractionation conditions.
289 The HF5-MALS analysis of AgNPs obtained with flow conditions described in section 2.5
290 is reported in Figure 1. The fractionation shows no void peak, expected at min 5, for the
291 unretained species (such as unreacted reagents for sample preparation or small species
292 dimensionally comparable to channel membrane cut-off), and a retained peak a t_R=8 min
293 typical for the nanostructure. An rms value of 45 nm was evaluated for the NPs, with an
294 hydrodynamic radius of about 23 nm, indicating an r_g /r_h ratio of 1.7 that is typical for rod
295 conformation; as deeper discussed in the next paragraph

296 It's also possible to observe that when the flow field ends ($t_R=17$ min) in the elution-
297 injection step only a small LS signal is evident so all eluted samples are separated during
298 the HF5 analysis. The presence of a small light scattering signal and a non significant UV
299 signal (data not shown) indicate that no NPs species are released at the end of the
300 fractionation method. As for sample polydispersity, in a homogeneous (i.e., monodisperse)
301 sample its average radius is independent from the averaging method. Then, the ratio
302 between values obtained with different methods will be equal 1 (i.e. polydispersity will
303 equal 1). If otherwise the sample contains a mixture of species of different gyration radii
304 (i.e., polydisperse sample) the average radius will depend on the averaging method and
305 the polydispersity will be different from 1. In this case, the calculated polydispersity
306 resulted to be 1.002, indicating that the nanoparticles are highly monodispersed.

307 HF5 shows good fractionation/characterization results for NPs using water as mobile
308 phase, having both a high reproducibility and a limited dilution of the sample; this allows
309 for the determination of AgNPs at low concentration and for the direct collection of
310 released metal and its quantification. For this purpose, in order to verify that cationic silver
311 totally exits from the channel membrane, a FIA analysis and an analysis with applied
312 cross-flow line were performed using the methods reported in Table 1. No UV signal at
313 205 nm was recorded when the field is applied, confirming that in the fractionation analysis
314 cationic silver is filtered through the membrane pores during the focus-injection step (data
315 not shown).

316 **3.2 Morphological analysis of AgNPs**

317 From the HF5-MALS analysis of AgNPs an accurate conformational analysis of samples
318 was performed.

319 In **HF5**, separation is performed between species presenting different diffusion
320 coefficients. Being the diffusion coefficient of a particle directly linked to its hydrodynamic
321 radius r_h , a first dimensional information is obtained. **MALS** detection, on the other hand,

322 allows for the calculation of particles' average mean square radius r_g , which depends on
323 particle shape and compactness. By correlating r_g and r_h it is possible to determine
324 particles shape; more in detail, a r_g/r_h ratio of 1.7 is typical for rod structures, while a ratio
325 of 0.77-0.8 is typical for random coils as PS standards are. Standard PS particles were
326 separated under the same flow conditions and mobile phase (water) in order to confirm the
327 RMS radius values obtained by HF5-MALS and have a direct comparison for
328 hydrodynamic radius.

329 In Figure 2 the HF5-MALS analysis of PS standards and AgNPs is reported. In the same
330 Figure the r_g values (determined from the MALS analysis) and r_h values (determined from
331 the HF5 analysis) are also reported. At 7 min AgNPs particles are eluted and an r_g of 45
332 nm was evaluated; while at 7.8 min the 50 nm PS standard is eluted ($r_h = 25.5$ nm, r_g
333 =20nm) and at 12 min the 102 nm PS standard is eluted ($r_h = 51$ nm, $r_g = 46$ nm).

334 A ratio of $r_g / r_h = 1.7$ was calculated suggesting a chain shape. The HF5-MALS
335 morphological analysis suggests the presence of small aggregates of Ag nanoparticles in
336 a chain arrangement, as confirmed also by TEM observation discussed in the subsequent
337 section 3.3.

338 A chain shape is not very common among these materials, although some synthesis
339 methods to form Ag nanowires in solution-phase and PVP presence have been presented
340 [30], but this could also be related to the lack of descriptivity obtainable with DLS, which
341 factors in the hydrodynamic radius alone, and TEM, where the analysis can be biased by
342 sample handling. In fact, being this morphology related to an aggregation state, a soft
343 technique like field-flow fractionation can show the real appearance of the sample since
344 there are no stabilizers (like surfactants or additives which constituted the formulate) and
345 stressful steps are avoided. A tendency to form chain-like aggregates is however
346 noticeable in TEM analyses, although it does not concern all the particles, as discussed in
347 paragraph 3.3.

348 3.3 Size characterization

349 Figures 3a and 3b the particle size distribution by Intensity and by Volume of AgNPs after
350 ultrafiltration obtained from DLS analysis are shown. From cumulants analysis, the mean
351 hydrodynamic diameter (or Z-average), r_h of AgNPs has been measured to be around 100
352 nm with a PDI of 0,24. However for samples characterized by a multimodal size
353 distribution, the Intensity particle size distribution should be considered for the assignment
354 of the size of each peak. AgNPs **sample shows a bimodal** size distribution with peaks
355 centered on 140 nm (Peak1, %PD=43) and **20 nm** diameter (Peak2, %PD=14). The
356 intensity size distribution are really sensitive to the presence of aggregates and large
357 particles, because scattered light intensity is proportional to the sixth power of their
358 diameter, thus to estimate the relative amount of each peak in the distribution, the Volume
359 particle size distribution has been considered. From this latter, the relative volume of the
360 two populations at 140 and 20 nm resulted almost the same, being respectively 49% and
361 51%.

362 Figure 4 shows the typical morphology and the distribution of AgNPs obtained from
363 transmission electron microscopy. The sample is polydisperse and the particle size
364 histogram follows a skewed Gaussian distribution with a long tail towards larger particle
365 size than the average particle size lying around 15-20 nm. Interestingly, the morphology
366 shows that while larger size aggregates (>40 nm, but on an average ~100 nm) are more or
367 less isolated the smaller size particles (<40 nm, but on an average ~15-20 nm) have a
368 tendency to be linked to the extent of forming a chain shape aggregate. The latter
369 observation agrees with data obtained from HF5-MALS method. The inherent nature of
370 the differences in sample state and preparation technique must be taken into account
371 when data from these entirely different techniques are compared especially for TEM for
372 which samples had to be sufficiently dry to allow this high vacuum microscopy technique,
373 pressure typically better than 10^{-6} Torr, to work.

374 **3.4 Ag release**

375 After the development of an HF5-MALS method for the characterization of AgNPs, its
376 potential as an analytical step useful to the study of biological impact of NPs through the
377 quantification of released metal in the environment was explored.

378 Purification from reagents of the AgNPs synthesis via membrane filtration during the
379 focus-injection step of the analysis, and determination of silver release from AgNPs were
380 then performed. A schematic view of the proposed method able to size separate NPs and
381 isolate cationic Ag fraction as described in section 2.7.2 is reported in Figure 5.

382 Some experiments were performed in HF5 system in order to define operative conditions
383 to quantify, with a good recovery, the ionic silver contained into a sample of nanoparticles
384 synthesized by an industrial process. As described in section 2.7 the standard solution of
385 AgNO_3 (1904 ppm) was analyzed with the HF5 method (cationic Ag collection) reported in
386 Table 1. Five aliquots of 3 ml were collected from cross-flow line and analyzed by FAAS.
387 For each one, silver concentration was obtained by interpolation of absorbance signal on
388 the calibration curve. FAAS measurements indicated that a volume of 12 mL must be
389 collected since silver content of the latter fractions was under the limit of detection (data
390 not shown). The results showed the recovery of cationic silver was higher than 90%
391 confirming that these conditions allow maximizing recovery of cationic silver collected from
392 the cross-flow line through HF5 membrane.

393 These experimental conditions were applied to dose cationic silver in a sample of AgNPs
394 diluted 1:10 from batch. FAAS measurements indicated that the ionic silver amount in the
395 sample is about 50% of the total. This value is consistent with the cationic Ag
396 concentration determined, by XRF analysis, in samples obtained after ultrafiltration
397 process, as reported in section 2.7.3.

398 Such result confirms the capability of HF5 technique in one-step process to separate ionic
399 phase from solid one, allowing for a better correlation between physicochemical properties

400 and biological reactivity. A more sound comprehension of nanospecific biological reactivity
401 in fact will support mechanistic studies and allow the control of nanophase reactivity by
402 playing with surface engineering (safety by design approach).

403

404 4. CONCLUSIONS

405 On-line coupling of /HF5 with MALS appears to be an ideal, hyphenated methodology for
406 the simultaneous size-separation and characterization of AgNPs samples because they
407 provide independent size information. The r_h values determined by AF4/HF5 can be
408 correlated to the r_g values determined by MALS and information on particle shape and
409 morphology can be obtained. All the analysis can be performed in aqueous media
410 providing fundamental information regarding the actual state of aggregation, size and
411 shape of nanoparticles in physiological media. This leads to more realistic assessment of
412 the risk posed by AgNPs to health, safety and the environment. In addition, the ability to
413 separate the Ag^+ ions from AgNPs during the size analysis can be advantageous in
414 providing further quantification of its potential risk, which largely originate from the release
415 of Ag^+ ions. Further studies will be conducted to create a suitable protocol for analysis of
416 metal release through fiber filtration. Overall, the combinatorial approach described in this
417 article may significantly improve the characterization of metal-based nanoparticles in order
418 to study both their functional effectiveness and potential hazards.

419

420 5. ACKNOWLEDGMENTS

421 The research leading to these results has received funding from the European
422 Community's Seventh Framework Programme (FP7/2007-2013) through the project
423 SANOWORK under Grant Agreement n. 280716. The HRTEM has been made available
424 under the INSPIRE programme, funded by Irish Government's Programme for Research in
425 Third Level Institutions, Cycle 4, National Development Plan 2007-2013, which is

426 supported by European Union Structural Fund. Drs. Abbasi Gandhi and Vishnu Mogili of
427 the University of Limerick are acknowledged for generating HRTEM data.

428

429 6. COMPETING INTEREST

430 Andrea Zattoni, Barbara Roda and Pierluigi Reschiglian are associates of the academic
431 spinoff company byFlow Srl (Bologna, Italy). The company mission includes know-how
432 transfer, development, and application of novel technologies and methodologies for the
433 analysis and characterization of samples of nano-biotechnological interest.

434

435

436 FIGURE CAPTIONS

437 Figure 1: HF5-MALS analyses of AgPVP nanoparticles in water. Light scattering signal at
438 90° and r_g values determined with MALS detector are reported.

439 Figure 2: HF5-MALS of AgPVP nanoparticles and PS. Light scattering signal at 90° and r_g
440 values determined with MALS detector are reported for AgNPs (gray lines) and PS
441 standards (brown lines).

442 Figure 3: DLS Particle size distribution by Intensity (a) and by Volume (b) for ultrafiltered
443 AgPVP nanoparticles dispersed in water at 0,13 mg/ml (pH = 4,5).

444 Figure 4: TEM micrograph (over) and a histogram of the mean diameter of sample AgNPs
445 after ultrafiltration (below).

446 Figure 5: Schematic view of an on-line, one-step Ag⁺ filtration and particles purification
447 with HF5: (a) Cationic Ag filtration during focus-injection and NPs relaxation, (b) AgNPs
448 size-separation and fractions collection.

449

450

451

452

453 REFERENCES

[1] US Nanotechnology Initiative, www.nano.gov/nni2.htm

[2] S.W.P. Wijnhoven, W.J.G.M. Peijnenburg, C.A. Herberts, W.I. Hagens, A.G. Oomen, E.H.W. Heugens, B. Roszek, J. Bisschops, I. Gosens, D. Van De Meent, S. Dekkers, W.H. De Jong, M. van Zijverden, A.J.A.M. Sips, R. E. Geertsma, Nano-silver – a review of available data and knowledge gaps in human and environmental risk assessment, *Nanotoxicology* 3(2) (2009) 109-138

-
- [3] SCENIHR (Scientific Committee on Emerging and Newly Identified Health Risks), Nanosilver: safety, health and environmental effects and role in antimicrobial resistance, 2014
- [4] M.N. Moore, Environmental Risk Management - the State of the Art Environment International 32(8) (2006) 967–976
- [5] P.H.M. Hoet, I. Brüske-Hohlfeld, O.V. Salata, Nanoparticles — known and unknown health risks, J. Nanobiotechnol. 2(12) (2004) 1-15
- [6] G.A. Sotiriou, S.E. Pratsinis, Antibacterial Activity of Nanosilver Ions and Particles, Environ. Sci. Technol. 44 (2010) 5649–5654
- [7] M. Auffan, J. Rose, M.R Wiesner, J-Y. Bottero, Chemical stability of metallic nanoparticles: A parameter controlling their potential cellular toxicity in vitro, Environmental Pollution 157(4) (2009) 1127–1133
- [8] X. Chen, H.J. Schluesener, Nanosilver: A nanoparticle in medical application, Toxicology Letters 176(1) (2008) 1–12
- [9] C.N.Lok, C.M. Ho, R. Chen, Q.Y. He, W.Y. Yu, H. Sun, P.K.H. Tam, J.F. Chiu, C.M. Che, Silver nanoparticles: partial oxidation and antibacterial activities, J. Biol. Inorg. Chem. 12 (2007) 527–534
- [10] EUROPEAN COMMISSION HEALTH & CONSUMER PROTECTION
DIRECTORATE-GENERAL Directorate C - Public Health and Risk Assessment C7 - Risk assessment; SCIENTIFIC COMMITTEE ON EMERGING AND NEWLY IDENTIFIED HEALTH RISKS (SCENIHR); The appropriateness of existing methodologies to assess the potential risks associated with engineered and adventitious products of nanotechnologies, 2005
- [11] Helmut Hinterwirth¹ Susanne K. Wiedmer, Maria Moilanen, Angela Lehner, Gunter Allmaier, Thomas Waitz, Wolfgang Lindner, Michael Lammerhofer Comparative method

evaluation for size and size-distribution analysis of gold nanoparticles *J. Sep. Sci.* 2013, 36, 2952–2961

[12] P.J. Wyatt. Light scattering and the absolute characterization of macromolecules, *Anal. Chim. Acta.* 272(1) (1993) 1–40

[13] P. Reschiglian, D.C. Rambaldi, A. Zattoni, Flow field-flow fractionation with multiangle light scattering detection for the analysis and characterization of functional nanoparticles, *Anal. Bioanal. Chem.* 399 (2011) 197-203

[14] J.C. Giddings, Field-flow fractionation: analysis of macromolecular, colloidal, and particulate materials, *Science* 260 (1993) 1456-1465

[15] D. Roessner, W.M. Kulicke, On-line coupling of flow field-flow fractionation and multi-angle laser light scattering, *J. Chromatogr. A* 687 (1994) 249-258

[16] H. Thielking, D. Roessner, W.M. Kulicke, Online Coupling of Flow Field-Flow Fractionation and Multiangle Laser Light Scattering for the Characterization of Polystyrene Particles, *Anal. Chem.* 67 (1995) 3229-3233

[17] P.J. Wyatt, Submicrometer particle sizing by multiangle light scattering following fractionation, *J. Colloid. Interf. Sci.* 197 (1998) 9-20

[18] A. Zattoni, D. Rambaldi, P. Reschiglian, M. Melucci, S. Krol, A. M. Coto Garcia, A. Sanz-Medel, D. Roessner, C. Johann, Asymmetrical flow field-flow fractionation with multi-angle light scattering detection for the analysis of structured nanoparticles, *J. Chromatogr. A* 1216 (2009) 9106-9112

[19] B. Schmidt, K. Loeschner, N. Hadrup, A. Mortensen, J. J. Sloth, C. Bender Koch, and E. H. Larsen., Quantitative Characterization of Gold Nanoparticles by Field-Flow Fractionation Coupled Online with Light Scattering Detection and Inductively Coupled Plasma Mass Spectrometry, *Anal. Chem.* 83, (2011), 2461–2468

-
- [20] L. Calzolari, D. Gilliland, C. Pascual García, F. Rossi, Separation and characterization of gold nanoparticle mixtures by flow-field-flow fractionation, *J Chrom A* 1218(27), (2011), 4234–4239
- [21] O. Geiss, C. Cascio, D. Gilliland, F. Franchini, J. Barrero-Moreno, Size and mass determination of silver nanoparticles in an aqueous matrix using asymmetric flow field flow fractionation coupled to inductively coupled plasma mass spectrometer and ultraviolet–visible detectors, *J Chrom A* 1321, (2013), 100–108
- [22] A. Zattoni, B. Roda, F. Borghi, V. Marassi, P. Reschiglian, Flow field-flow fractionation for the analysis of nanoparticles used in drug delivery., *J. Pharm. Biomed. Anal.* 87 (2014) 53-61
- [23] P. Reschiglian, B. Roda, A. Zattoni, M. Tanase, V. Marassi, S. Serani, Hollow-fiber flow field-flow fractionation with multi-angle laser scattering detection for aggregation studies of therapeutic proteins, *Anal. Bioanal. Chem.* 406(6) (2014) 1619-1627
- [24] P. Reschiglian, A. Zattoni, L. Cinque, B. Roda, F. Dal Piaz, A. Roda, M.H. Moon, B.R. Min, On-Line Hollow-Fiber Flow Field-Flow Fractionation-Electrospray Ionization/Time-of-Flight Mass Spectrometry of Intact Proteins, *Anal. Chem.* 76 (2004) 2103-2111
- [25] A. Roda, D. Parisi, M. Guardigli, A. Zattoni, P. Reschiglian, Combined approach to the analysis of recombinant protein drugs using hollow-fiber flow field-flow fractionation, mass spectrometry, and chemiluminescence detection, *Anal. Chem.* 78 (2006)1085-1092
- [26] A. Zattoni, D.C: Rambaldi, B. Roda, D. Parisi, A. Roda, M.H. Moon, P. Reschiglian, Hollow-fiber flow field-flow fractionation of whole blood serum, *J. Chromatogr. A* 1183 (2008) 135-142
- [27] A. Zattoni, D.C. Rambaldi, S. Casolari, B. Roda, P. Reschiglian, Tandem hollow-fiber flow field-flow fractionation, *J Chrom A.* 1218(27), (2011), 4132-4137

[28] A. Zattoni, S. Casolari, D.C. Rambaldi, P. Reschiglian, Hollow-Fiber Flow Field-Flow Fractionation, *Curr. Anal. Chem.* 3(4) (2007) 310-323

[29] C. Johann, S. Elsenberg, U. Roesch, D.C. Rambaldi, A. Zattoni, P. Reschiglian, A novel approach to improve operation and performance in flow field-flow fractionation, *J. Chromatogr. A* 1218 (2011) 4126-4131

[30] X. Gu, C. Nie, Y. Lai, C. Lin, Synthesis of silver nanorods and nanowires by tartrate-reduced route in aqueous solutions, *Materials Chemistry and Physics* 96 (2006) 217–222

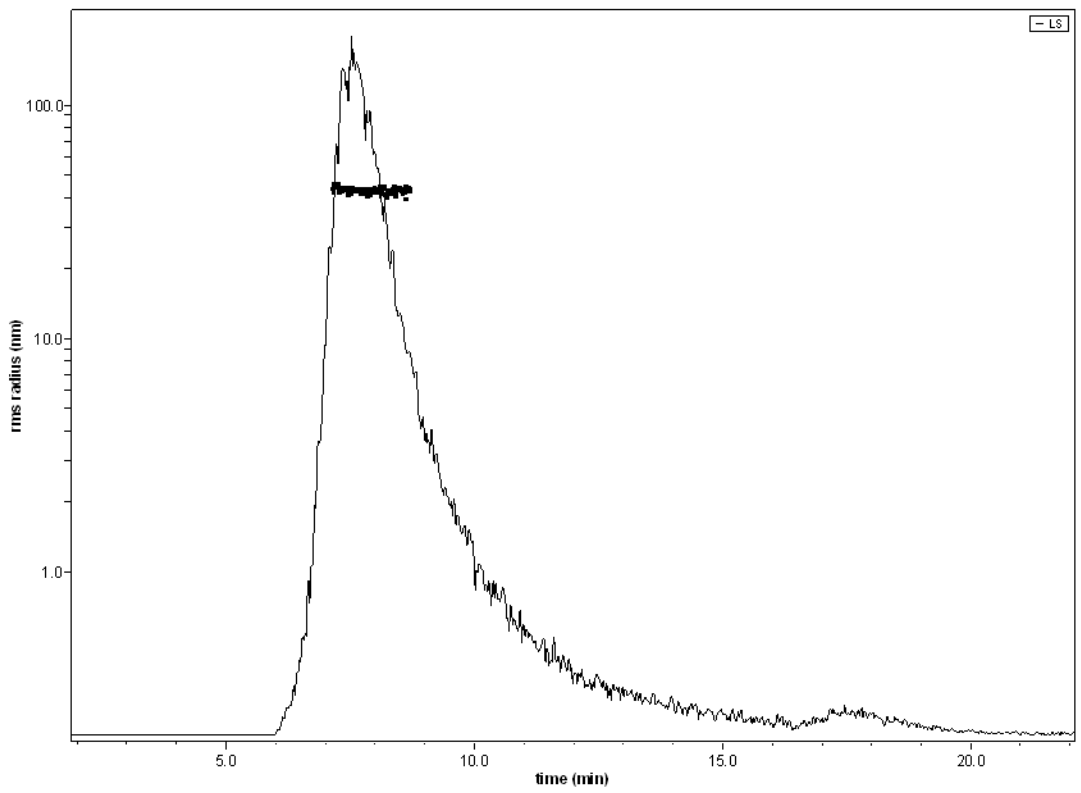


Figure 1

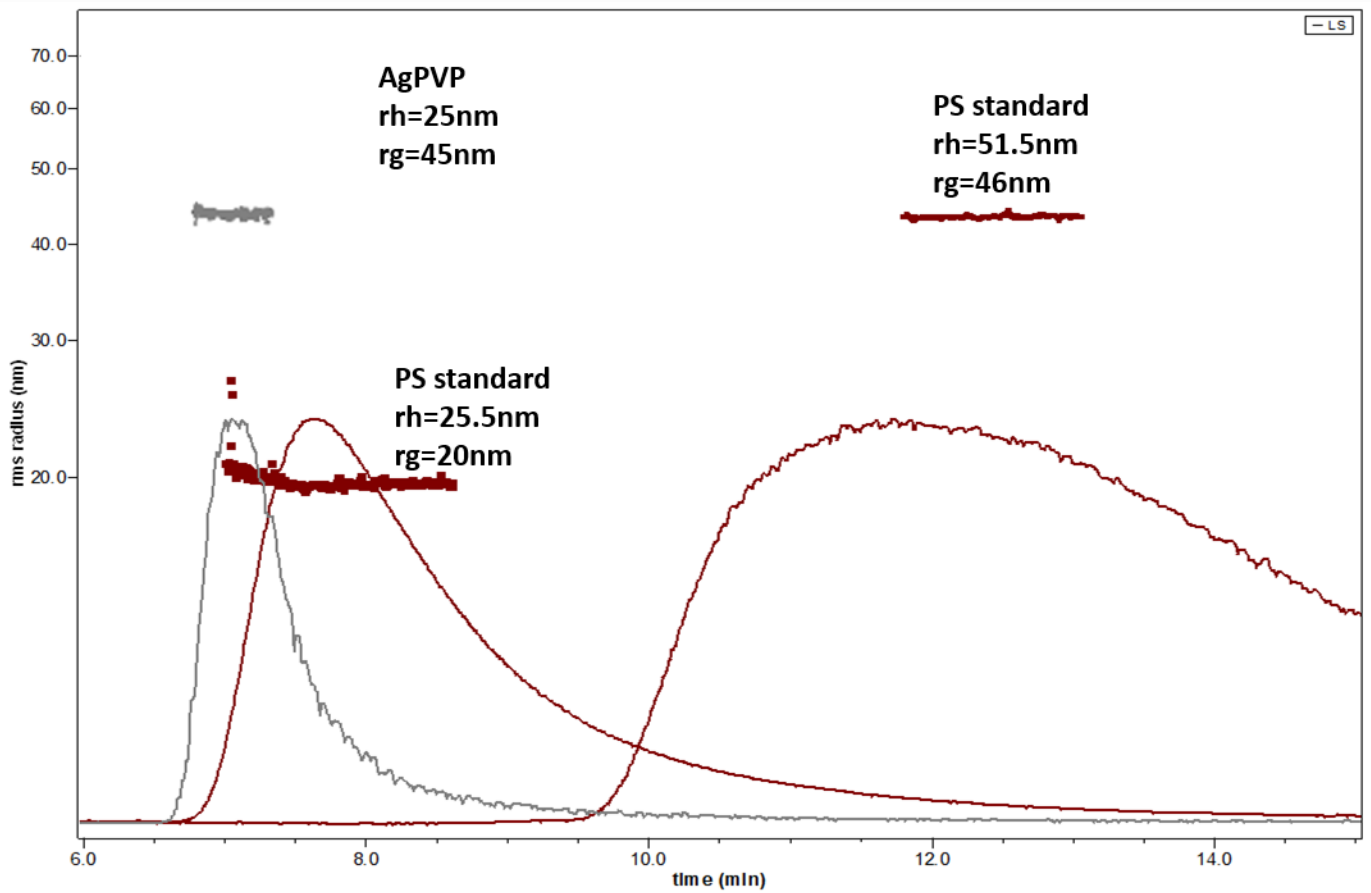


Figure 2

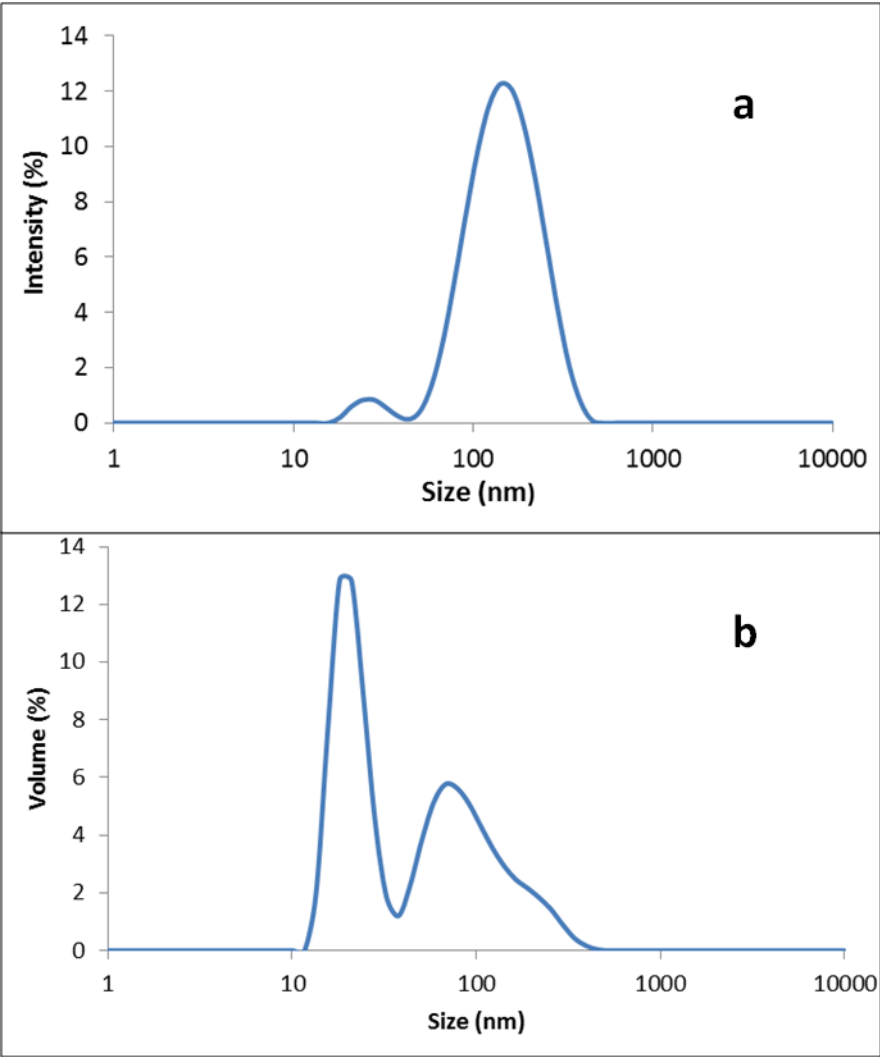


Figure 3

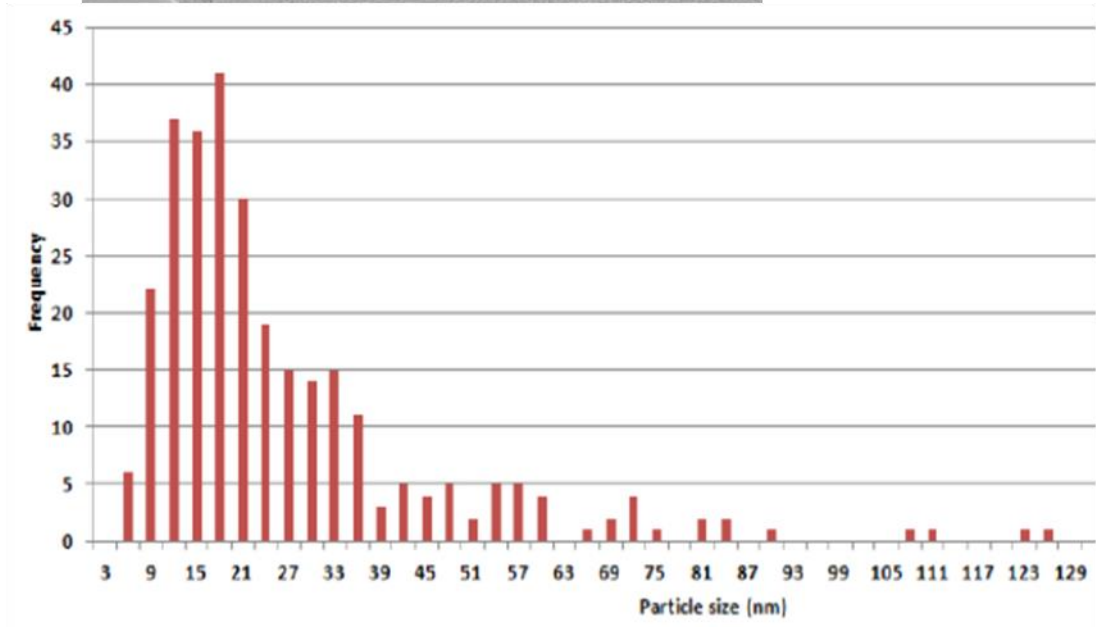
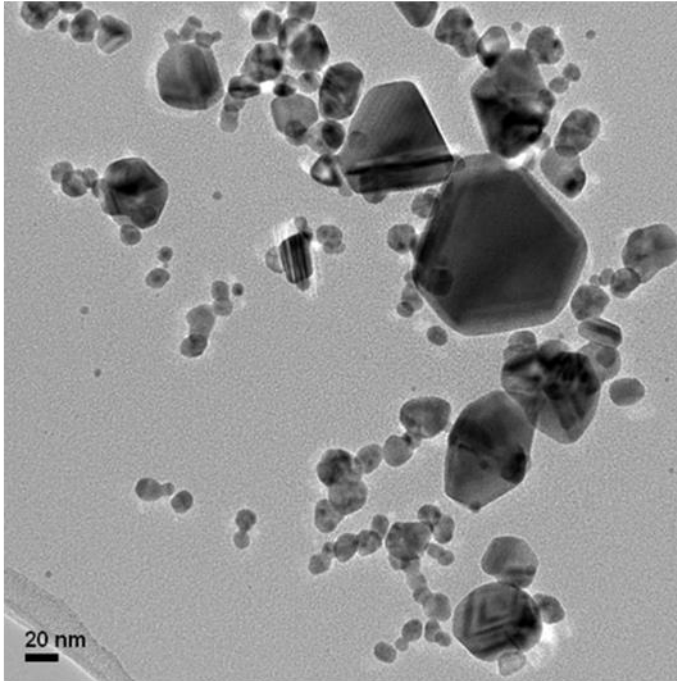


Figure 4

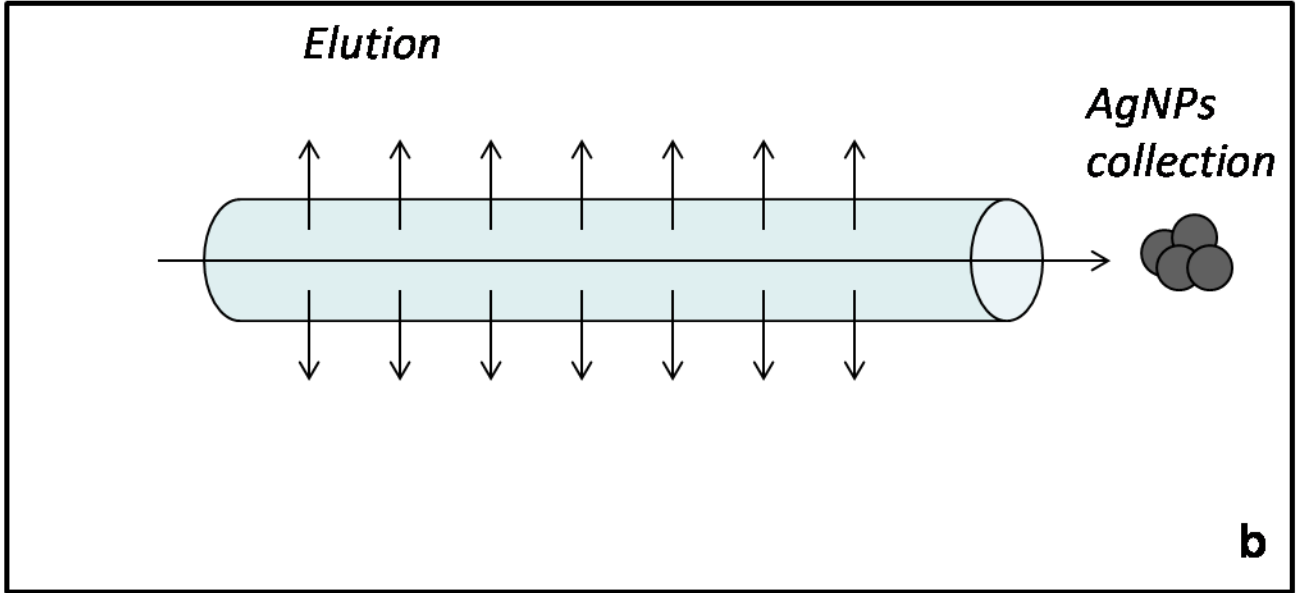
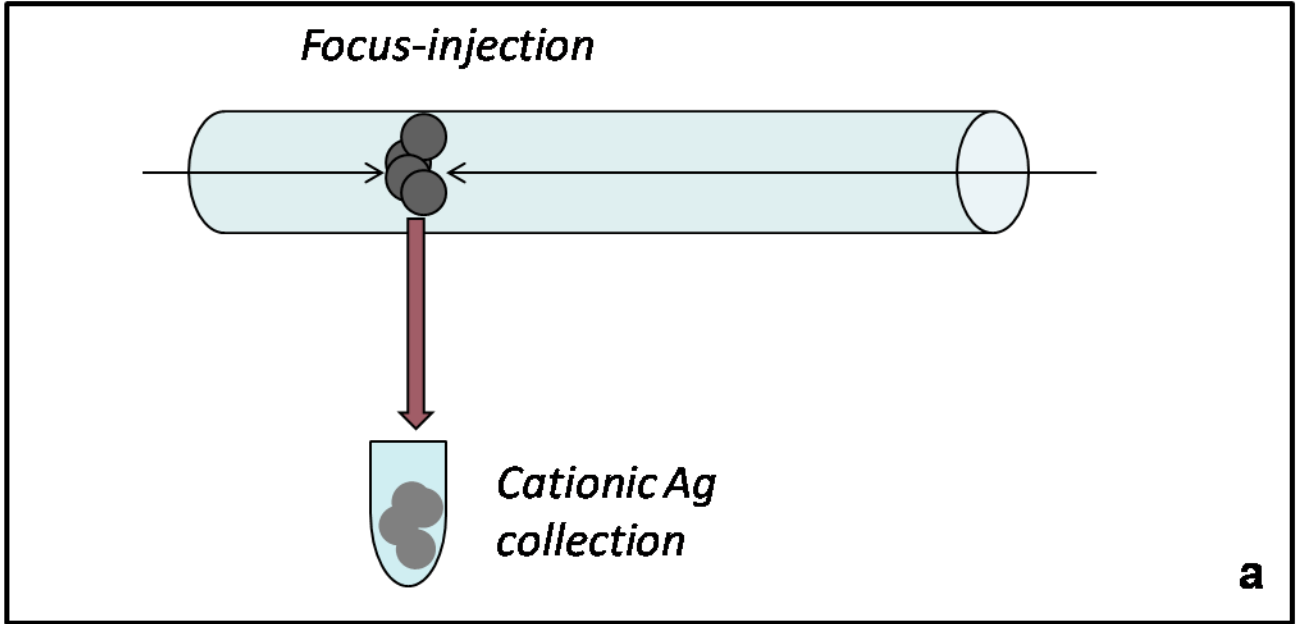


Figure 5